EARTHQUAKE ENGINEERING AND STRUCTURAL DYNAMICS, VOL. 25, 945–963 (1996)

CONVEX MODEL FOR SEISMIC DESIGN OF STRUCTURES—II: DESIGN OF CONVENTIONAL AND ACTIVE STRUCTURES

S.-R. TZAN† AND C. P. PANTELIDES*

Department of Civil Engineering, 3220 Merrill Engineering Building, University of Utah, Salt Lake City, UT 84112, U.S.A.

SUMMARY

The optimal design of the members of conventional structures or structures equipped with active bracing systems, known as active structures, is presented for uncertain excitations. Three approaches are used for obtaining the optimal structural design: (1) the time-history analysis of an actual earthquake record (AR), (2) the global energy-bound convex model adjusted with an excitation-specific reduction factor (RGEB), and (3) the global energy-bound convex model adjusted with an average reduction factor (ARGEB) for a set of excitations with common characteristics. The optimal structures obtained using the RGEB and ARGEB convex models have different sizes for their conventional members from the designs based on a time-history analysis of the actual earthquake (AR). The optimal design of the structure is carried out using a modified annealing algorithm. The advantage of using convex models to perform the optimization is that they represent a more general excitation than a single earthquake record. In addition, the RGEB and ARGEB convex models require considerably less computational effort since the constraints of the optimization become time-independent. A comparison between optimal designs of structures with conventional members only, and active structures indicates that the latter are more efficient by combining the conventional and active members.

KEY WORDS: active structure; active bracing system; convex model; optimal structural design; seismic excitation; simulated annealing method

INTRODUCTION

Active structures are structural systems which are composed of two types of load-resisting members: (a) conventional static members such as beams and columns that are designed to support static design loads; and (b) active members such as active mass dampers, active braces, or active variable stiffness members that are designed to resist dynamic loads such as those that a structure may experience in a strong earthquake. The concept of the active structure has important implications for the design of new structures in seismic regions that are to be equipped with active systems. The new structure must be designed to utilize efficiently both the properties of the conventional static members and the dynamic properties of the active members. Recent progress in the area of active structural control has brought the application of active systems from theory and experiment to actual implementation.[1,2]

The concept of the active structure was studied by Soong and Manolis.[3] A structure was designed optimally in terms of minimizing structural volume while simultaneously the optimal control force for the active control system was obtained. The structural volume in this context is a measure of the structure's cost. The structural design variables were defined as the member areas, and the control variables were the optimal control forces. The general theory of optimal control of parametric systems was used to formulate the active structure optimization solution. The formulation resulted in a system of non-linear coupled equations whose solution was accomplished iteratively using non-linear programming and steepest descent methods.

---

†Research Assistant
*Associate Professor

CCC 0098–8847/96/090945–19

Received 6 February 1995
Revised 5 October 1995

The design of active structures was also addressed by Cheng and Pantelides,[4] and Pantelides,[5] who formulated the solution in two stages: (a) the optimal control forces were expressed in closed form as implicit functions of the design variables (equivalent to the moments of inertia of the structural members); and (b) the design variables were modified iteratively in order to minimize the structural volume with constraints imposed on the structural displacements, frequencies, and maximum level of control forces. The definition of the active structure can be extended to include in addition to the active control systems not only purely static members,[3] but also passive control members such as viscoelastic dampers.[6] The design methods for active structures, developed in References 3–5, use a time-dependent record of a past earthquake or an artificial earthquake acceleration as the excitation which is known in advance; the resulting computational effort required for the optimization process is rather costly since the constraints are time-dependent. This situation is common in the structural optimization not only of active structures but also of conventional structures designed for earthquakes.[7-9]

Design optimization has seen an increase since the advent of the computer in the last half-century. Automated optimization originated from many fields and several methods have been proposed.[10,11] Optimization algorithms include: (1) mathematical programming, (2) optimality criteria, (3) approximation,[12,13] and (4) global search methods. Global search methods use random sequences of designs and include genetic algorithms which emulate the natural selection process of nature and operate on a principle of survival of the fittest,[14] and simulated annealing algorithms that emulate the reduction of the temperature in a bar that goes from a high to a low temperature.[15]

Optimization techniques have focused primarily on structural optimization of systems with static constraints. When dynamic or time-varying constraints are imposed, the feasible region becomes disjoint and local minima are possible. Cassis[16] described this phenomenon in detail for planar frames subjected to horizontal vibrations at their foundation. Estimates for the maximum number of disjoint feasible regions in the optimization of structural systems subjected to harmonic loads have also been developed.[17-19] In the area of minimum weight design of damped structures subjected to dynamic loads, Cassis and Schmit[20] discussed the disjoint nature of the feasible region for some combinations of constraints and loadings. A solution of the dynamic constraints problem based on upper-bound approximations for the behaviour constraints was developed by Mills-Curran and Schmit.[19]

The simulated annealing method, which provided a new perspective on traditional optimization problems, involves random sequences of candidate designs with a probabilistic acceptance criterion of a better design at each subsequent iteration. Ackley[21] developed the Iterated Simulated Annealing (ISA) method and the Stochastic Hill-Climbing (SHC) method. In the SHC method the probability evaluation of a new design is held constant for the duration of the search. In the ISA method the probability evaluation of a new design starts at a high value of an adjustable parameter determining the acceptability of the design (temperature) and is reduced by a decay rate during the search. Several applications of the simulated annealing method exist in the literature.[22-24]

The method proposed in this paper seeks to replace the dynamic optimization of either traditional deterministic structures or active structures by a simpler static optimization. This can be achieved if the time-dependent displacements, member stresses, and control forces could be replaced by a maximum value representing an upper bound of the structural response to the earthquake. This is done by using estimates of the maximum response from energy-bound convex models.[25] In addition, the convex model estimates represent the structure's response to a more general excitation than a single earthquake record. The design of the active structure is extended to include uncertain excitations using energy-bound convex models.[25] Records from past earthquakes are considered in the optimal design of structures with or without active bracing systems. A simulated annealing algorithm[26] is used for the optimization of conventional as well as active structures.

STRUCTURAL OPTIMIZATION

The structural optimization problem for a building subjected to an earthquake is a dynamic one and is formulated as follows. Find the optimal parameters ($\bar{A}$), which are the cross-sectional areas of the conventional

static structural members, that minimize the structural volume $V(\mathbf{A})$ subject to displacement constraints on the structural response, $\mathbf{x}(t)$, stress constraints on the structural members, $\boldsymbol{\sigma}(t)$, and side constraints on the design variables, $\mathbf{A}_L$ and $\mathbf{A}_U$. The subscript L denotes the lower bound and subscript U is the upper bound of the design variable. The minimization of the structural volume as the objective represents a measure of the cost of the conventional structure. Mathematically, this can be expressed as

$$\min \quad V(\mathbf{A}) \tag{1}$$

$$\text{s.t.} \quad \delta x_j(\mathbf{A}, t) \leqslant \delta x_{\text{all},j} \quad j = 1, \ldots, \bar{j}, \quad t \geqslant 0 \tag{2a}$$

$$\sigma_k(\mathbf{A}, t) \leqslant \sigma_{\text{all},k} \quad k = 1, \ldots, \bar{k}, \quad t \geqslant 0 \tag{2b}$$

$$A_L \leqslant A_k \leqslant A_U, \quad k = 1, \ldots, \bar{k}, \quad t \geqslant 0 \tag{2c}$$

where $\delta x_{\text{all},j}$ is the allowable interstorey drift of the jth floor of the structure, and $\bar{j}$ is the number of nodes at which displacement constraints are imposed; $\sigma_{\text{all},k}$ is the allowable combined stress in a structural member, and $\bar{k}$ is the number of structural members.

Note that if the maximum values of the structural response are used, the quantities on the left-hand side of equations (2a) and (2b) become time-independent and the optimization problem is reduced to a static one. Estimates of the maximum structural response can be obtained using the global energy-bound convex model adjusted with either a reduction factor (RGEB) or an average reduction factor (ARGEB).[25] The static optimization problem has the objective of minimizing the structural volume given in equation (1) subject to the constraints

$$\delta x_{j,\max}(\mathbf{A}) \leqslant \delta x_{\text{all},j}, \quad j = 1, \ldots, \bar{j} \tag{3a}$$

$$\sigma_{k,\max}(\mathbf{A}) \leqslant \sigma_{\text{all},k}, \quad k = 1, \ldots, \bar{k} \tag{3b}$$

and also subject to the side constraints of equation (2c). In equation (3a), $\delta x_{j,\max}$ is the estimate of the maximum interstorey drift of the jth floor of the structure obtained by the convex model. In equation (3b), $\sigma_{k,\max}$ is the estimate of the maximum combined stress of the kth member of the structure obtained by the convex model. It is obvious that the solution of the static optimization problem of equations (1), (3a), (3b), and (2c) is much easier than that of the original dynamic problem, because the constraints are time-independent.

A modified annealing method is used for obtaining the optimal structural design.[26] In this method, the design variables are determined by a random reference number that is requested by the program based on the time of the computer clock. The new candidate design is accepted with a probability, p, determined by[21]

$$p = \frac{1}{1 + e^{(V_a - V_c)/T}} \tag{4}$$

where V_a is the candidate value of the objective, V_c is the current value of the objective, and T is the temperature. The 'temperature' is an adjustable parameter; larger values of T cause the probability of acceptance of the candidate design to reach a 50 per cent acceptance rate. Two improvements were implemented in the modified annealing method to make it suitable for the present optimization problem:[26] (1) reduction of the search range; when one candidate relative minimum value of the objective is found, the search range is reduced to exclude points outside an enlarged region which contains the relative minimum; and (2) sensitivity analysis; if a given displacement violates the constraint, the neighbouring structural members are identified by sensitivity analysis[27] and the area of those members is increased, the increase being determined randomly. These improvements are advantageous in dynamically constrained problems where the feasible region is disjoint. By contrast, standard optimization methods were not always able to find sequential feasible designs because of the disjoint feasible region.[26]

The structural analysis of frame-type buildings considered here is carried out using the direct stiffness method, with a capability for computing and enforcing a strength ratio of column to beam equal to or greater than unity. The strength ratio of column to beam is necessary in order to enforce the strong column-weak beam philosophy of the design codes.[28] The design variables are the cross-sectional areas of the structural

members; their second moments of area, I, can be obtained using well-known relations as follows:[10]

$$I_i = Z_i \times s_i$$
$$Z_i = \beta_i \left(\frac{A_i}{\alpha_i}\right)^{3/2}, \quad s_i = \chi_i \left(\frac{A_i}{\alpha_i}\right)^{1/2} \tag{5}$$

where Z_i, s_i, and A_i are the section modulus, the least radius of gyration, and the cross-sectional area of the ith element respectively, and the constants α_i, β_i, and χ_i for wide-flange steel sections equal 0·58, 0·58, and 0·67, respectively. In what follows, the dynamic and static optimization problems are solved for conventional as well as active structures.

Example 1— conventional structure

A ten-storey frame with conventional static members only, as shown in Figure 1 is optimized by performing analyses in the time domain using dynamic constraints. The design variables are the cross-sectional areas of the beams and columns of the frame. Variable linking is implemented so that only eight design variables are used, as shown in Figure 1(b). The lumped mass procedure is used for solution of the dynamic equations of motion. An inherent structural damping level is assumed at 5 per cent of critical for all modes. The allowable combined stress for each member is assumed as 150 MPa, and the allowable drift for each floor is set at $h/180$, which equals 2·54 cm for the first floor and 2·00 cm for floors above the first. The strong-column weak-beam philosophy is implemented by forcing the strength ratio of column to beam to be equal to or greater than unity, which reflects code requirements for earthquake design. In addition, elastic response of the frame is assumed throughout the iteration history. In this section, the optimal design of the ten-storey frame without active control is presented. Two excitations, the S00E component of the 18 May 1940 El-Centro earthquake, and the S16E component of the 17 February 1971 San Fernando earthquake are considered.

Optimal design of conventional structure for 1940 El-Centro earthquake. The optimal design using the time-history response for the 1940 El-Centro earthquake (AR) and the optimal designs for the global energy-bound convex model adjusted with the excitation-specific reduction factor (RGEB),[25] and the average reduction factor (ARGEB)[25] are shown in Table I. The values shown for stress and drift are the maxima obtained at the final design. The active constraints for each optimal design are shaded in Table I. The reduction factor for the RGEB convex model is excitation-specific and can be used only for the 1940 El-Centro earthquake (S00E component). The average reduction factor for the ARGEB convex model is the average value of the reduction factors from 26 California records[25] (subset S7 of Table IV in Reference 25).

The minimum volume obtained by the RGEB convex model is 3·3 per cent less than that obtained by using the time-history analysis of the actual record (AR). The result obtained by using the ARGEB convex model is 49 per cent more than that obtained by the AR procedure. From the definition of the global energy-bound convex model adjusted with the average reduction factor (ARGEB),[25] the result obtained in Table I for the ARGEB convex model could be used for any other excitation in California which has the same global energy bound as the 1940 El-Centro earthquake.

The time-history analysis of three earthquake records and that for the 1940 El-Centro earthquake are used to verify the designs obtained using the AR procedure and the ARGEB convex model (see Table I). A scaled record of the S16E component of the 1971 San Fernando earthquake, the S90N component of the 1994 Northridge earthquake (Santa Monica City Hall), and an artificial earthquake (Figure 2), all having the same global energy bound as the 1940 El-Centro earthquake, are considered. The peak acceleration, duration, and global energy bound of the four excitations are shown in Table II. Note that the artificial earthquake is created using a sinusoidal function multiplied by the amplitude envelope function[29] of Figure 3. The artificial ground acceleration is expressed as

$$\ddot{x}_g(t) = bf(t) \sum_{k=1}^{25} \bar{a}_k \sin(\bar{\omega}_k t) \tag{6a}$$

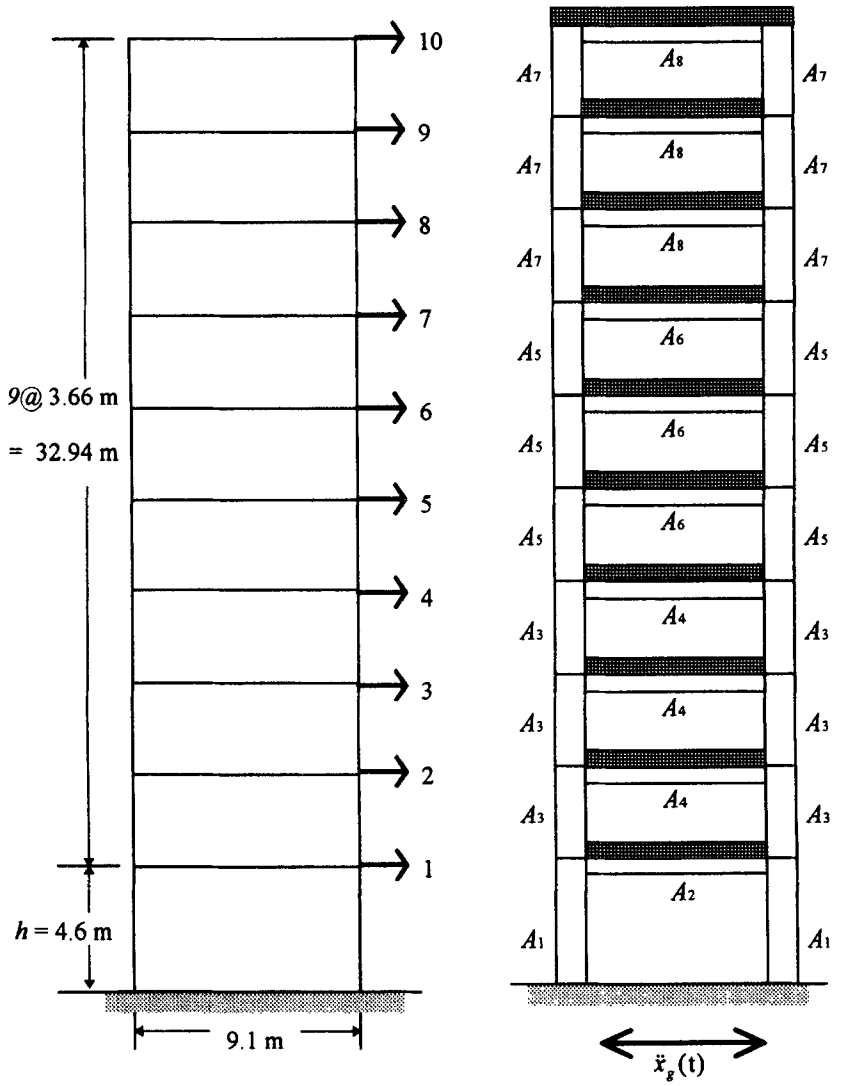

$A_1, \ldots, A_8$ = Area of Frame Member
1, ..., 10 = No. of DOF
Lumped Mass = 34,034 kg for each floor

(a) (b)

Figure 1. Ten-storey frame: (a) dimensions and degrees-of-freedom, (b) loading and design variables

$$f(t) = \begin{cases} t^2/4, & 0 \leqslant t \leqslant 2 \\ 1, & 2 \leqslant t \leqslant 17{\cdot}5 \\ e^{[-0{\cdot}07153(t-17{\cdot}5)]}, & 17{\cdot}5 \leqslant t \leqslant 40 \\ 0{\cdot}05 + 0{\cdot}00375(60-t)^2, & 40 \leqslant t \leqslant 60 \end{cases} \tag{6b}$$

Table I. The optimal design of the ten-storey conventional structure subjected to the 1940 El-Centro earthquake

Frame group	Cross-sectional area (cm^2)				Combined stress for beam (MPa)			Combined stress for column (MPa)			Interstorey drift (cm)		
	AR	RGEB	ARGEB	Fl.	AR	RGEB	ARGEB	AR	RGEB	ARGEB	AR	RGEB	ARGEB
A1	448·31	603·52	820·57	1	84·98	88·86	103·55	118·21	112·71	138·82	1·35	1·21	1·22
A2	379·26	292·64	598·10	2	92·49	100·26	124·99	77·31	79·22	109·09	1·72	1·64	1·79
A3	430·38	529·49	694·98	3	87·77	92·25	125·91	64·52	63·14	88·60	1·80	1·68	1·99
A4	375·54	453·80	574·74	4	85·75	80·88	119·23	53·63	50·18	76·98	1·89	1·50	1·98
A5	402·90	278·79	667·91	5	90·13	88·75	110·24	60·34	87·19	69·26	1·99	1·94	1·92
A6	360·52	263·78	551·26	6	88·82	78·42	99·42	55·44	55·89	59·98	1·97	1·98	1·81
A7	353·38	267·66	429·92	7	80·92	75·55	91·74	49·71	42·79	47·31	1·87	1·84	1·67
A8	310·48	253·01	351·54	8	70·64	78·74	95·76	43·92	48·20	70·19	1·98	1·94	1·95
Volume (cm^3)	6 232 048	6 028 142	9 285 281	9	53·27	70·22	76·98	39·63	49·60	51·65	1·76	1·93	1·90
				10	32·73	47·14	49·80	26·32	41·87	35·98	1·24	1·51	1·42

Note: AR, Maximum response using the time history of the actual record; RGEB, global energy-bound convex model adjusted with the excitation-specific reduction factor[25]; ARGEB, global energy-bound convex model adjusted with the average reduction factor from subset 7 (S7) of Table IV in Reference 25

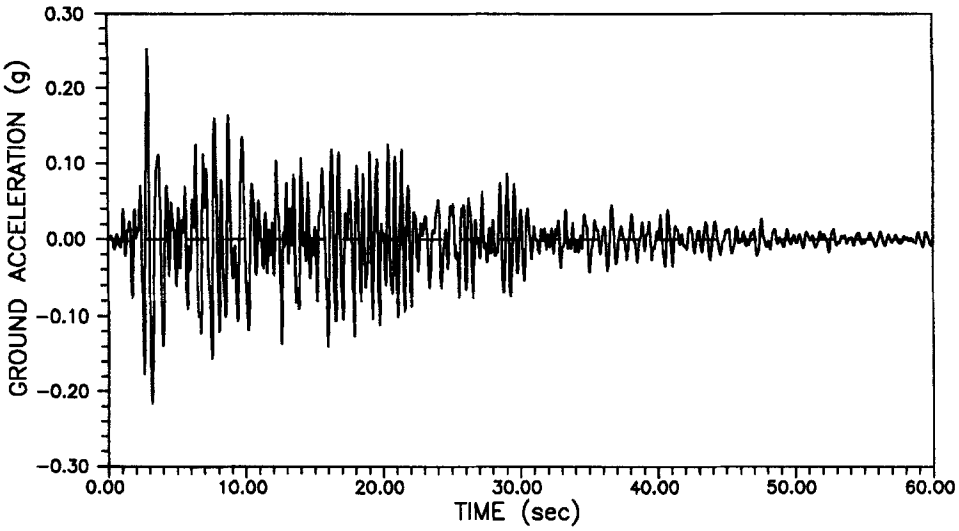

Figure 2. Artificial earthquake using an amplitude envelope function

Table II. Peak acceleration and global energy-bound of the excitations for verifying the structure designed by the ARGEB convex model of subset S7 (Reference 25)

Excitations	Peak acceleration (g)	Duration (sec)	Global energy bound (m^2/sec^3)
1940 El-Centro	0·348	53·0	11·38
Scaled San Fernando	0·545	41·0	11·38
Scaled Northridge	0·706	60·0	11·38
Artificial earthquake	0·252	60·0	11·38

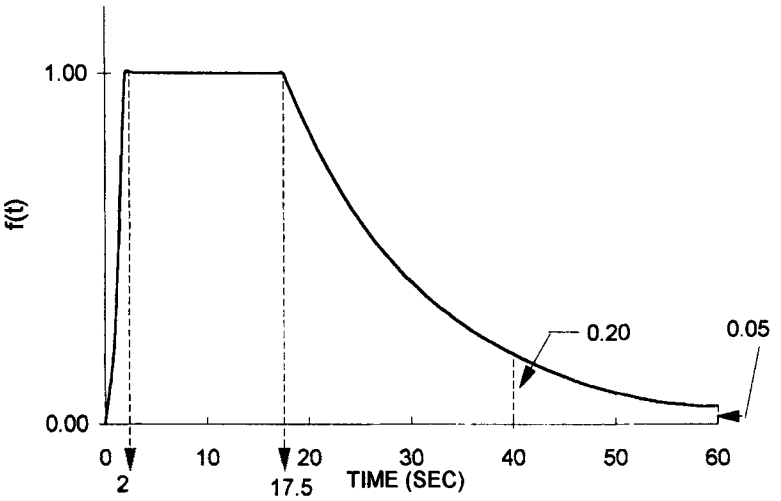

Figure 3. Time-dependent variation of amplitude envelope function for artificial earthquake

where $\bar{a}_k$ and $\bar{\omega}_k$ are the values of the 25 highest peak amplitudes and frequencies chosen from the 1940 El-Centro earthquake record; and b is a constant chosen to give the same global energy bound as the 1940 El-Centro earthquake. The function $f(t)$ in equation (6b) has been modified from that of Reference 29, so that the earthquake duration of these records is comparable. It should be noted that the artificial excitation of Figure 2 was not used in the evaluation of the reduction factors of the ARGEB convex model.

Figure 4(a) shows the interstorey drift response for the structure designed using the time-history of the actual 1940 El-Centro earthquake record (Building I); Figure 4(b) shows the interstorey drift response for the structure designed by the ARGEB convex model (Building II). It can be observed that Building I exceeds the allowable drift at all floors for the scaled record of the 1971 San Fernando earthquake, and at seven floors for the scaled record of the 1994 Northridge earthquake. The maximum drift of Building I is 84 and 36 per cent more than the allowable drift when the structure is subjected to the scaled records of the San Fernando and Northridge earthquakes. Building II which was designed by the ARGEB convex model has a better response

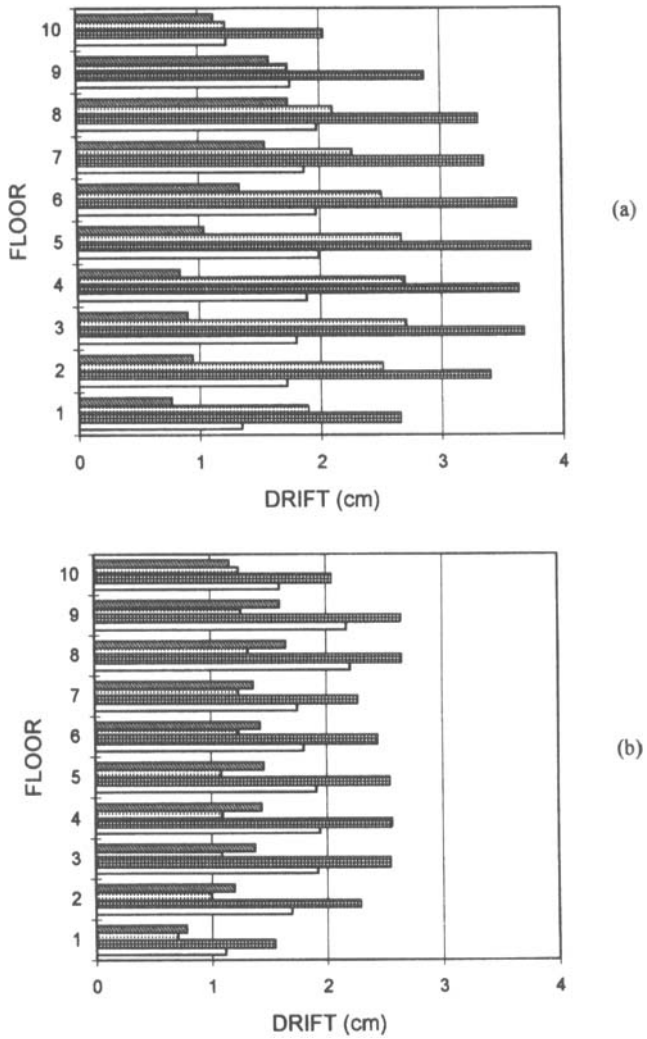

Figure 4. Interstorey drift of the ten-storey frame: (a) AR design for 1940 El-Centro of Table I (Building I) and (b) ARGEB convex model design of Table I (Building II); (▨) artificial earthquake shown in Figure 2; (□) scaled record of 1994 Northridge earthquake; (■) scaled record of 1971 San Fernando earthquake; (□) 1940 El-Centro earthquake record

than Building I for both scaled records. The maximum drift is only 32 and 11 per cent larger than that of the allowable drift in the scaled record of the San Fernando earthquake and the actual record of the 1940 El-Centro earthquake. It should be noted that the drift response to the artificial earthquake of Figure 2 for both Buildings I and II remains within the allowable limits.

Optimal design of conventional structure for 1971 San Fernando earthquake. The optimal design for the actual record of the 1971 San Fernando earthquake and the optimal designs using the RGEB and ARGEB convex models are listed in Table III. The reduction factor used in the RGEB convex model is excitation-specific, valid only for the 1971 San Fernando earthquake (S16E component). The average reduction factor used in the ARGEB convex model was obtained from the 12 records of the 1971 San Fernando and 1994 Northridge earthquakes (subset S6 of Table IV in Reference 25). The active constraints for each optimal design are shown shaded in Table III.

The minimum volume obtained by the RGEB convex model is 2·0 per cent more than that obtained from the time history of the actual record (AR). The minimum volume obtained by the ARGEB convex model is 54 per cent more than that obtained by the AR procedure. It can also be observed that the minimum volume of the structure designed for the 1971 San Fernando is 2·2 times larger than that for the 1940 El-Centro earthquake shown in Table I, which is approximately equal to the square root of the ratio of the global energy bounds for these two earthquakes.

The structure designed by the AR procedure (referred to as Building III) and the ARGEB convex model (referred to as Building IV) are also verified by a dynamic analysis for the 1971 San Fernando and scaled 1994 Northridge earthquakes shown in Table IV. Figure 5 shows the interstorey drift of the structures subjected to the actual record of the 1971 San Fernando earthquake, and the scaled record of the 1994 Northridge earthquake with the same global energy bound. It can be observed that Building III has much larger drifts than Building IV when the structures are subjected to the scaled record of the 1994 Northridge earthquake. The maximum drifts are 76 and 12 per cent larger than the allowable drift for Buildings III and IV. Figures 4 and 5 show that, in general, the structures designed by the ARGEB convex model respond well for other excitations which have the same global energy bound. However, this is not true for structures designed for a single earthquake.

ACTIVE CONTROL SYSTEM

Significant progress has been made in recent years in the application of control theory to civil structures.[2] In the present paper, an active bracing system (ABS) as shown in Figure 6 is used in the development of the active structure. The ABS has been studied both theoretically and experimentally and has been tested successfully on a full-scale structure.[30] The optimal control forces from the ABS can be obtained using techniques which have been established specifically for civil structures, such as the standard quadratic performance index for the linear quadratic regulator (LQR) given as[31]

$$J = \frac{1}{2}\int_0^{t_f} [\mathbf{z}^{\mathrm{T}}(t)\mathbf{Q}\mathbf{z}(t) + \mathbf{u}^{\mathrm{T}}(t)\mathbf{R}\mathbf{u}(t)]\,\mathrm{d}t \tag{7}$$

in which t_f is the earthquake duration, $\mathbf{z}^{\mathrm{T}}(t)$ is the transpose of the state vector $\mathbf{z}^{\mathrm{T}}(t) = \{\mathbf{x}(t), \dot{\mathbf{x}}(t)\}^{\mathrm{T}}$, where $\mathbf{x}(t)$ and $\dot{\mathbf{x}}(t)$ are the relative displacement and velocity response of the structure, and $\mathbf{Q}$ and $\mathbf{R}$ are the weighting matrices chosen by the designer.

The optimal control force, $\mathbf{u}^*(t)$, can be obtained by minimizing J subject to the constraint of the equation of motion which in its state form can be expressed as

$$\dot{\mathbf{z}}(t) = \mathbf{A}\mathbf{z}(t) + \mathbf{B}\mathbf{u}(t) + \mathbf{H}\ddot{X}_g(t) \tag{8a}$$

$$\mathbf{A} = \left[\begin{array}{c|c} \mathbf{O} & \mathbf{I} \\ \hline -\mathbf{M}^{-1}\mathbf{K} & -\mathbf{M}^{-1}\mathbf{C} \end{array}\right], \qquad \mathbf{B} = \left[\begin{array}{c} \mathbf{O} \\ \hline \mathbf{M}^{-1}\mathbf{b} \end{array}\right] \qquad \mathbf{H} = \left[\begin{array}{c} \mathbf{O} \\ \hline \mathbf{M}^{-1}\beta \end{array}\right] \tag{8b}$$

Table III. The optimal design of the ten-storey conventional structure subjected to the 1971 San Fernando earthquake

Frame group	Cross-sectional area (cm^2)			Fl.	Combined stress for beam (MPa)			Combined stress for column (MPa)			Interstorey drift (cm)		
	AR	RGEB	ARGEB		AR	RGEB	ARGEB	AR	RGEB	ARGEB	AR	RGEB	ARGEB
A1	1534·31	1587·42	2649·55	1	100·69	106·38	78·80	132·40	143·99	126·41	0·91	0·95	0·54
A2	876·97	900·01	2508·64	2	142·31	139·56	115·88	148·39	145·77	149·10	1·65	1·60	1·01
A3	962·99	1002·77	1588·74	3	145·12	146·20	133·12	115·01	118·69	120·79	1·95	1·94	1·45
A4	839·02	834·34	1241·68	4	134·45	140·03	135·51	97·36	98·57	98·85	1·93	1·99	1·60
A5	906·10	926·20	1239·37	5	118·34	126·80	130·44	86·54	95·91	112·47	1·84	1·95	1·73
A6	782·88	834·10	1173·85	6	96·08	112·25	118·68	73·27	80·00	92·61	1·73	1·81	1·70
A7	606·58	643·84	977·81	7	77·80	103·31	112·96	48·21	62·18	71·23	1·66	1·68	1·62
A8	572·07	523·38	660·66	8	78·47	109·95	124·43	63·31	83·98	89·30	1·97	1·94	1·89
Volume (cm^3)	13 656 970	13 933 900	21 097 000	9	68·61	89·43	106·71	46·49	59·67	57·90	1·88	1·92	1·96
				10	52·77	59·35	76·38	45·74	42·30	41·74	1·39	1·49	1·59

Note: ARGEB, global energy-bound convex model adjusted with the average reduction factor from subset 6 (S6) of Table IV in Reference 25

Table IV. Peak acceleration and global energy bound of the excitations for verifying the structure designed by the ARGEB convex model of subset S6 (Reference 25)

Excitations	Peak acceleration (g)	Duration (sec)	Global energy bound (m^2/sec^3)
1971 San Fernando	0·172	41·0	52·61
Scaled Northridge	1·517	60·0	52·61

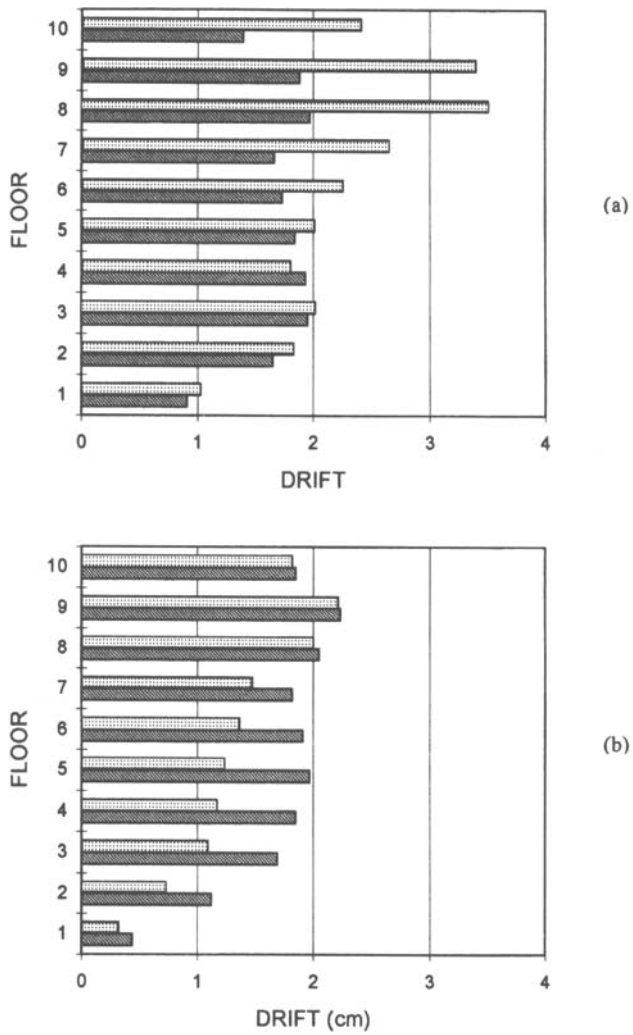

Figure 5. Interstorey drift of the ten-storey frame: (a) AR design for 1971 San Fernando of Table III (Building III) and (b) ARGEB convex model design of Table III (Building IV); (□) scaled record of 1994 Northridge earthquake; (▨) 1971 San Fernando earthquake record

where **M**, **C** and **K** are the $N \times N$ mass, damping, and stiffness matrices, N being the number of degrees of freedom; **O** and **I** are the null and identity matrices; **b** is an $N \times m$ matrix which defines the ABS locations with respect to the structure's topology, m being the number of controllers, $\boldsymbol{\beta}$ is the effective loading vector which for earthquake excitations is $\boldsymbol{\beta}^T = \{-m_1, -m_2, \ldots, -m_N\}$ where m_i is the mass of ith floor; and $\ddot{X}_g(t)$ is the

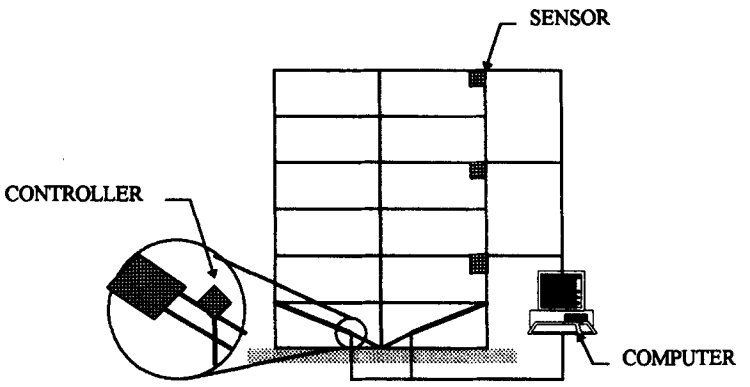

Figure 6. Active bracing system

ground base-acceleration. The result of the minimization of J in equation (7) is given by

$$\mathbf{u}^*(t) = -\tfrac{1}{2}\mathbf{R}^{-1}\mathbf{B}^{\mathrm{T}}\mathbf{P}(t)\mathbf{z}(t) \tag{9a}$$

$$\mathbf{PA} + \mathbf{A}^{\mathrm{T}}\mathbf{P} - \tfrac{1}{2}\mathbf{PBR}^{-1}\mathbf{B}^{\mathrm{T}}\mathbf{P} - 2\mathbf{Q} = \mathbf{0} \tag{9b}$$

The unknown matrix $\mathbf{P}(t)$ can be found by assuming that it is constant with respect to time from equation (9b). Matrix $\mathbf{Q}$ could be assigned to be any positive-semidefinite matrix. One way of simplifying the control procedure is to define $\mathbf{Q} = \mathbf{I}$, the identity matrix. Weighting matrix $\mathbf{R}$ is assigned to be an identity matrix multiplied by a constant r.

A time-dependent performance index, $J(t)$, defined for instantaneous optimal control (IOC),[32] can also be used to obtain the optimal control forces. The index can be expressed as

$$J(t) = \mathbf{z}^{\mathrm{T}}(t)\mathbf{QZ}(t) + \mathbf{u}^{\mathrm{T}}(t)\mathbf{Ru}(t) \tag{10}$$

The optimal control forces, $\mathbf{u}^*(t)$, are obtained by minimizing $J(t)$ subject to the constraint of the equation of motion of the dynamic system. The weighting matrices, $\mathbf{R}$ and $\mathbf{Q}$, can either be assigned to be a diagonal and an identity matrix or they can be determined by the Lyapunov method.[6] If the weighting matrix $\mathbf{R}$ in equation (10) is assumed to be diagonal with elements $R_{i,i} = R$, $\mathbf{Q}$ is assumed to be an identity matrix, and if $\mathbf{M}$ is assumed to be symmetric, the optimal control forces can be derived as[32]

$$\mathbf{u}^*(t) = \frac{-\Delta t}{2R}\mathbf{b}^{\mathrm{T}}\mathbf{M}^{-1}\mathbf{x}(t) \tag{11}$$

where Δt is the integration time step. The optimal control forces in equation (11) constitute a velocity feedback control algorithm. Substituting equation (11) into equation (8a) yields

$$\mathbf{M}\ddot{\mathbf{x}}(t) + \mathbf{C}^*\dot{\mathbf{x}}(t) + \mathbf{Kx}(t) = \boldsymbol{\beta}\ddot{X}_{\mathrm{g}}(t) \tag{12a}$$

$$\mathbf{C}^* = \mathbf{C} + \mathbf{C}_{\mathrm{ABS}} \tag{12b}$$

$$\mathbf{C}_{\mathrm{ABS}} = \frac{\Delta t}{2R}\mathbf{bb}^{\mathrm{T}}\mathbf{M}^{-1} \tag{12c}$$

where $\mathbf{C}_{\mathrm{ABS}}$ is the equivalent damping matrix due to the presence of the active control. Equation (12) can be used to obtain the response of a structure equipped with an ABS during a horizontal earthquake. The structural response of an actively controlled structure in the time domain can be obtained from either equations (8a) or (12a). Note that either the LQR or the IOC method can be used to determine the response of a structure with an active bracing system which was discussed in Reference 6. In this paper, the IOC method of equation (12) is used.

For simulation purposes the ground acceleration, $\ddot{X}_g(t)$, is not known before the earthquake occurs. However, in the structural optimization of conventional or active structures it is not necessary to have available the entire time history of the structural response; estimates of the peak values of the response are sufficient. This observation makes the use of convex models attractive since the estimates of the peak response obtained from the convex models can be used to formulate the constraints in the optimization process.

For the global energy-bound (GEB) convex model, the quantities required to obtain the response estimate in the case of an actively controlled structure are: the effective damping ratios (ξ_i^*), the frequencies, and mode shapes of the controlled structure, and the global energy bound, $E_{GEB}(\infty)$, of the earthquake.[25] The effective damping can be obtained from equation (12b) as

$$\mathbf{\Phi}^T\mathbf{C}^*\mathbf{\Phi} = \begin{bmatrix} 2\omega_1\xi_1^* & & & 0 \\ & \ddots & & \\ & & 2\omega_i\xi_i^* & \\ & & & \ddots \\ 0 & & & 2\omega_N\xi_N^* \end{bmatrix} \tag{13}$$

where $\mathbf{\Phi}$ is the modal matrix of the structure. The global energy bound is a given value for a certain excitation or is assumed for an earthquake which has not occurred yet. The modal displacement, velocity, and acceleration can be determined by replacing the inherent structural damping of equation (5) of Reference 25 with the effective damping, ξ_i^*; the maximum response in physical co-ordinates can be approximated by the square root of the sum of the squares (SRSS) of the modal responses given by equation (6) of Reference 25. Once the maximum velocity, $\dot{\mathbf{x}}_{max}$, is obtained the estimate of the control force using the GEB convex model can be determined from equation (11) as

$$|\mathbf{u}_{max}^*| = \left| \frac{-\Delta t}{2R} \mathbf{b}^T\mathbf{M}^{-1}\dot{\mathbf{x}}_{max} \right| \tag{14}$$

The ten-storey frame shown in Table I of Reference 25 is used to examine the RGEB and ARGEB convex models for the active bracing systems (ABS). One ABS is assumed to be installed on the first floor and one on the second floor of the building. Note that in this application the ABS is used in the form of a retrofit. The maximum responses obtained from the time history of the actual record (AR), and the RGEB and ARGEB convex models are shown in Table V. The reduction factor used in the RGEB convex model is excitation-specific for the 1940 El-Centro earthquake. The average reduction factor used in the ARGEB convex model is obtained from 26 California records.[25] The same control parameters are used in the three methods. Note that the control force is affected only by the velocity of the floors as shown in equation (14). It can be observed that the ratio of the estimated control forces obtained from the RGEB and ARGEB convex models to the maximum control forces obtained from the actual time history (AR), is approximately equal to the ratio of the velocity of the same floors at the two levels where the ABS are installed.

Example 2 — Active structure

In this section the optimal design of an active structure with one active bracing system (ABS) on the first floor and one ABS on the second floor of the ten-storey frame is presented. Two actual earthquake records are used to design the ten-storey active structure stated above. The control force is constrained to a maximum of 20 per cent of the excitation's effective lateral force. The effective lateral force is determined by multiplying the total mass of the structure by the peak acceleration of the excitation.

Optimal design of active structure for 1940 El-Centro earthquake. Table VI shows the optimal design using the time-history analysis of the 1940 El-Centro earthquake record, the RGEB convex model with the excitation-specific reduction factor, and the ARGEB convex model with the average reduction factor from 26 California records (subset S7 of Reference 25). It can be observed that the minimum volume obtained by the

Table V. Maximum response of the ten-storey frame with two ABS for the 1940 El-Centro earthquake record

Floor	AR	RGEB	RGEB/AR	ARGEB	ARGEB/AR
Displacement (cm)					
1	1·17	1·46	1·25	1·96	1·68
2	2·78	3·37	1·21	4·61	1·66
3	4·59	5·35	1·17	7·47	1·63
4	6·42	7·17	1·12	10·25	1·60
5	8·21	8·80	1·07	12·88	1·57
6	9·85	10·24	1·04	15·28	1·55
7	11·28	11·56	1·02	17·40	1·54
8	12·59	12·88	1·02	19·38	1·54
9	13·64	14·06	1·03	21·01	1·54
10	14·36	14·93	1·04	22·16	1·54
Velocity (cm/sec)					
1	7·09	10·50	1·48	11·93	1·68
2	15·66	21·53	1·37	25·84	1·65
3	22·83	31·44	1·38	39·39	1·73
4	30·86	38·88	1·26	51·22	1·66
5	38·90	44·07	1·13	61·55	1·58
6	45·89	48·03	1·05	70·74	1·54
7	51·84	52·10	1·01	79·23	1·53
8	56·10	57·78	1·03	88·02	1·57
9	61·54	64·80	1·05	96·52	1·57
10	68·29	71·24	1·04	103·43	1·51
Acceleration (cm/sec^2)					
1	296·35	274·22	0·93	238·18	0·80
2	449·10	406·01	0·90	336·62	0·75
3	542·59	506·83	0·93	427·86	0·79
4	501·20	555·66	1·11	496·43	0·99
5	423·77	554·20	1·31	535·34	1·26
6	407·42	547·83	1·34	573·28	1·41
7	424·85	530·55	1·25	602·33	1·42
8	536·72	565·65	1·05	661·22	1·23
9	631·80	664·82	1·05	737·32	1·17
10	697·33	791·09	1·13	816·16	1·17
Maximum control force (kN)					
1	138	204	1·48	232	1·68
2	171	218	1·28	275	1·61

RGEB convex model is 0·7 per cent more than that obtained by using the time history of the actual record (AR) for the 1940 El-Centro earthquake. The minimum volume obtained by the ARGEB convex model is 64 per cent more than that of the AR design. However, note that compared to the design of the structure without structural control the present designs required, on the average, 15 per cent less volume.

The performance of the structure designed by the time history of the actual El-Centro earthquake record (Building V) and the structure designed by the ARGEB convex model (Building VI) are examined using a time-history analysis of the four excitations shown in Table II with the same global energy bound. The same control parameters are used in the design of Buildings V and VI. The interstorey drifts for these two buildings are shown in Figure 7. Similar results are obtained as observed in Figures 4 and 5. Building VI responds much better than Building V for all excitations, especially for the scaled record of the San Fernando earthquake. The maximum control forces of both ABS in Buildings V and VI are, on average, 19 and 11 per cent of the excitation effective lateral force, respectively.

Table VI. The optimal design of the ten-storey active structure subjected to the 1940 El-Centro earthquake

Frame group	Cross-sectional area (cm^2)			Fl.	Combined stress for beam (MPa)			Combined stress for column (MPa)			Interstorey drift (cm)		
	AR	RGEB	ARGEB		AR	RGEB	ARGEB	AR	RGEB	ARGEB	AR	RGEB	ARGEB
A1	379·16	469·75	729·38	1	87·92	82·73	101·90	114·75	101·41	130·27	1·51	1·27	1·26
A2	323·01	349·48	517·62	2	94·35	96·16	121·47	69·58	71·14	87·96	1·88	1·77	1·80
A3	373·55	416·75	699·09	3	90·56	93·62	123·31	55·02	56·15	70·07	1·96	1·88	1·99
A4	317·52	337·33	494·67	4	85·93	87·95	117·92	54·09	48·85	60·62	1·87	1·80	1·99
A5	358·61	288·81	565·16	5	75·62	87·25	108·67	49·29	66·41	68·65	1·78	1·99	1·99
A6	312·28	273·02	474·99	6	65·18	80·27	97·81	40·42	53·62	59·24	1·71	1·97	1·86
A7	254·21	276·60	418·48	7	58·31	75·81	90·79	33·11	42·96	46·56	1·64	1·84	1·72
A8	192·23	189·40	300·22	8	58·95	77·57	88·25	36·69	42·02	58·95	1·98	1·95	1·93
Volume (cm^3)	5 061 958	5 098 602	8 317 064	9	54·51	69·42	76·75	27·06	33·87	52·69	1·96	1·99	1·91
				10	41·79	51·40	52·99	26·82	28·70	31·74	1·43	1·61	1·47

	Maximum control force (kN)		
Floor	AR	RGEB	ARGEB
1	215	240	255
2	268	258	274

Note: ARGEB, Global energy-bound convex model adjusted with the average reduction factor from subset 7 (S7) of Reference 25

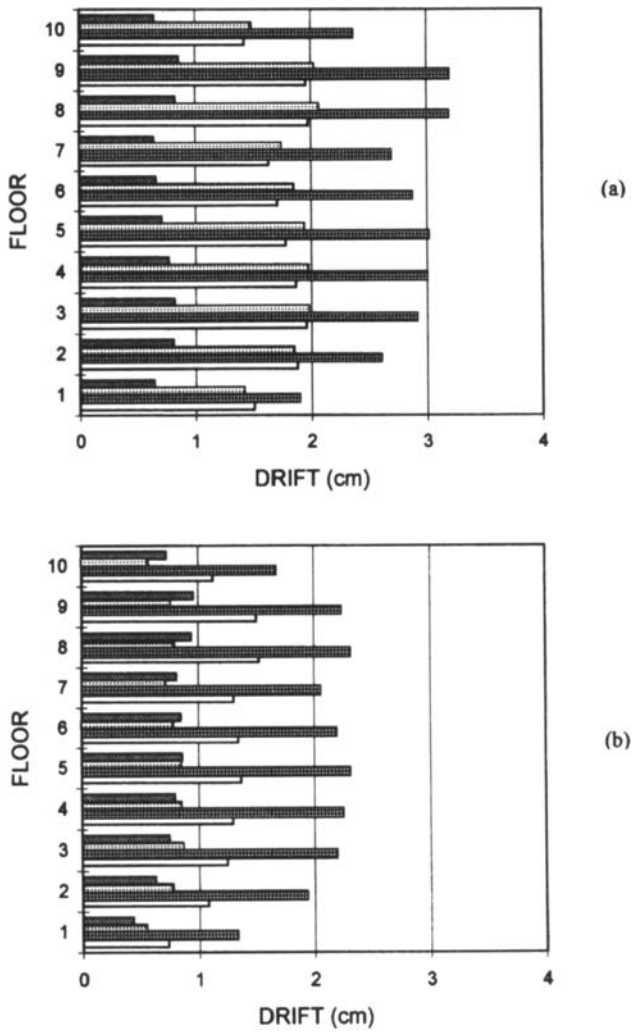

Figure 7. Interstorey drift of the ten-storey frame with two ABS: (a) AR design for 1940 El-Centro of Table VI (Building V) and (b) ARGEB convex model design of Table VI (Building VI); (▨) artificial earthquake shown in Figure 2; (□) scaled record of 1994 Northridge earthquake; (■) scaled record of 1971 San Fernando earthquake; (□) 1940 El-Centro earthquake record

Optimal design of active structure for 1971 San Fernando earthquake. Table VII shows the optimal designs for the 1971 San Fernando earthquake. The minimum volume obtained by the RGEB convex model is 3·3 per cent less than the minimum volume for the actual record (AR) for the 1971 San Fernando earthquake. For the results obtained by the ARGEB convex model, the subset S6 of Reference 25 is used in Table VII. The minimum volume results obtained by the ARGEB convex model is 59 per cent more than the minimum volume obtained using the actual record (AR) for the San Fernando earthquake.

This result, as well as that obtained for the conventional structure, indicates that in general the results obtained by the RGEB convex model are closer to those of the time history of the actual record (AR). The results obtained by the ARGEB convex model are further away as compared to the RGEB convex model from those of the AR procedure. However, the ARGEB convex model results are on the conservative side and within reasonable margins. In general, the structures designed by the ARGEB convex model respond better to other excitations than the structures designed by the time-history analysis for a specific excitation. The computational advantage of using convex models is obvious in the case of buildings with a large number of design variables, such as tall buildings. In that case, the calculations involved in obtaining the active structure

Table VII. The optimal design of the ten-storey active structure subjected to the 1971 San Fernando earthquake

Frame group	Cross-sectional area (cm^2)			Fl.	Combined stress for beam (MPa)			Combined stress for column (MPa)			Interstorey drift (cm)		
	AR	RGEB	ARGEB		AR	RGEB	ARGEB	AR	RGEB	ARGEB	AR	RGEB	ARGEB
A1	1381·40	1407·94	2669·11	1	108·98	82·75	82·84	145·86	112·07	122·42	1·03	0·77	0·59
A2	851·02	876·57	1509·07	2	142·77	116·13	114·76	141·93	120·07	134·59	1·71	1·36	1·05
A3	963·76	946·37	1649·58	3	145·21	122·99	126·14	112·64	95·60	109·77	1·97	1·67	1·36
A4	824·69	772·24	1290·17	4	137·05	118·36	130·86	95·00	79·12	92·57	1·96	1·72	1·49
A5	847·65	856·55	1144·00	5	125·29	108·93	142·75	92·05	77·79	131·28	1·96	1·70	1·81
A6	767·52	752·44	1030·03	6	109·19	97·67	136·96	77·81	66·18	97·59	1·82	1·60	1·93
A7	604·43	486·74	1083·07	7	97·68	90·49	129·73	58·69	51·60	78·70	1·65	1·49	1·87
A8	446·27	443·23	669·73	8	100·30	106·16	125·76	72·59	94·38	71·12	1·92	1·94	1·95
Volume (cm^3)	12 935 580	12 512 670	20 530 980	9	78·80	85·75	101·11	47·97	65·55	52·69	1·94	1·97	1·90
				10	53·37	53·05	77·09	33·29	44·62	37·24	1·49	1·45	1·55

	Maximum control force (kN)		
Floor	AR	RGEB	ARGEB
1	572	992	1147
2	1037	632	312

Note: ARGEB-Global energy-bound convex model adjusted with the average reduction factor from subset 6 (S6) of Reference 25

using the time-history analysis of the actual record are quite expensive. However, the convex model solutions could be obtained with less effort because of the static nature of the constraints.

CONCLUSIONS

The optimal design of conventional as well as active structures using the energy-bound convex models yields static member sizes that are different from those obtained using the actual earthquake record. The minimum volume required for conventional or active structures by the average reduction factor convex model (ARGEB) is approximately 50 per cent larger than the volume required by the optimal structure designed for a single earthquake record. One advantage of using convex models to perform the structural optimization is that they represent a more general excitation than a single earthquake. Thus, the structures designed using the ARGEB convex model respond well for other excitations with the same global energy bound; by contrast, structures designed for a specific earthquake record do not respond as well for other earthquakes. This is true for either conventional or active structures. Another advantage of using convex models is that the computational effort required for the optimization when using the energy-bound convex models is much less than that required when using actual earthquake records.

The optimal design of the active structure yields a minimum volume, on average, ten per cent less than the structural volume of the conventional structure. In this respect, active structures are seen to be more efficient by combing the conventional static members with the active members.

ACKNOWLEDGEMENTS

Financial support by the National Science Foundation under Grant No. MSS-9207252 is gratefully acknowledged. The authors would like to thank the reviewers for their comments.

REFERENCES

1. T. Kobori, 'Future direction on research and development of seismic response controlled structure', Position paper, *Proc. 1st world conf. struct. control*, Los Angeles, CA, 1994, pp. panel-19-31.
2. G. W Housner, T. T. Soong and S. F. Masri, 'Second generation of active structural control in civil engineering', Position paper, *Proc. 1st world conf. struct. control*, Los Angeles, CA, 1994, pp. panel-3-18.
3. T. T. Soong and G. D. Manolis, 'Active structures', *J. struct. eng. ASCE* **113**, 2290–2302 (1987).
4. F. Y. Cheng and C. P. Pantelides, 'Combining structural optimization and structural control', *Technical Report NCEER 88-0006*, State University of New York, Buffalo, NY, January 1988.
5. C. P. Pantelides, 'Optimum design of actively controlled structures', *Earthquake eng. struct. dyn.* **19**, 583–596 (1990).
6. S-R. Tzan and C. P. Pantelides, 'Hybrid structural control using viscoelastic dampers and active control systems', *Earthquake eng. struct. dyn.* **23**, 1369–1388 (1994).
7. M. A. Bhatti and K. S. Pister, 'A dual critical approach for optimal design of earthquake-resistant structural systems', *Earthquake eng. struct. dyn.* **9**, 557–572 (1981).
8. R. J. Balling, K. S. Pister and V. Ciampi, 'Optimal seismic-resistant design of a planar steel frame', *Earthquake eng. struct. dyn.* **11**, 541–556 (1983).
9. K. Z. Truman and D. J. Petruska, 'Parametric optimal design of steel structures', *Proc. 10th world conf. earthquake eng.*, Madrid, Spain, 1992, pp. 4453–4458.
10. E. J. Haug and J. S. Arora, *Applied Optimal Design*, Wiley, New York, 1979.
11. L. A. Schmit, 'Structural synthesis — its genesis and development', *AIAA J.* **19**, 1249–1263 (1981).
12. H. J. Kelley, 'The cutting plane method for solving complex programs', *SIAM J.* **8**, 703–712 (1960).
13. G. N. Vanderplaats, *Numerical Optimization Techniques for Engineering Design: With Applications*, McGraw Hill, New York, 1984.
14. E. D. Goldberg, *Genetic Algorithms in Search, Optimization and Machine Learning*, Addison-Wesley, Reading, MA, 1989.
15. S. Kirkpatrick, C. D. Jr. Gelatt and M. P. Vecchi, 'Optimization by simulated annealing', *Science* **220**, 671–680 (1983).
16. J. H. Cassis, 'Optimum design of structures subjected to dynamic loads', *UCLA-ENG-7451*, UCLA School of Engineering and Applied Science, Los Angeles, CA, 1974.
17. E. H. Johnson, 'Disjoint design spaces in the optimization of harmonically excited structures', *AIAA J.* **14**, 259–261 (1976).
18. E. H. Johnson, P. Rizzi, H. Ashley and S. A. Segenreich, 'Optimization of continuous one-dimensional structures under steady harmonic excitation', *AIAA J.* **14**, 1690–1698 (1976).
19. W. C. Mills-Curran and L. A. Schmit, 'Structural optimization with dynamic behavior constraints', *AIAA J.* **23**, 132–138 (1985).
20. J. H. Cassis and L. A. Jr. Schmit, 'Optimal structural design with dynamic constraints', *J. struct. eng. ASCE* **102** (ST10), 2053–2071 (1976).
21. D. H. Ackley, 'An empirical study of bit vector function optimization', in D. Lawrence (ed.), *Genetic Algorithms and Simulating Annealing*, Norgan Kaufmann, Los Altos, CA, 1987, pp. 170–271.

22. M. Salama, R. Bruno, G.-S. Chen and J. Garba, 'Optimal placement of excitations and sensors by simulated annealing', *NASA/Air Force Symposium on recent experiences in multidisciplinary analysis and optimization*, Hampton, VA, September 1988.
23. G.-S. Chen, R. J. Bruno and M. Salama,'Optimal placement of active/passive members in truss structures using simulated annealing', *AIAA J.* **29**, 1327–1334 (1991).
24. R. J. Balling, 'Optimal steel frame design by simulated annealing', *J. struct. eng. ASCE* **117**, 1780–1795 (1991).
25. C. P. Pantelides and S.-R. Tzan, 'Convex model for seismic design of structures — I: analysis', *Earthquake eng. struct. dyn.* **25**, 927–944 (1996).
26. S.-R. Tzan and C. P. Pantelides, 'An annealing strategy for optimal structural design', *J. struct. eng. ASCE* **122**(7), 815–827 (1996).
27. D. E. Grierson, 'Structural analysis for structural design', in F. Y. Cheng, *Proc. 11th analysis and computation conference: ASCE, structures congress '94 and IASS int. symp. '94*, Atlanta, GA, 24–28 April 1994, pp. 133–144.
28. International Conference of Building Officials, *Uniform Building Code, Vol. 2*, Whittier, CA, 2.362, 1994.
29. P. C. Jennings, G. W. Housner and N. C. Tsai, 'Simulated earthquake motions for design purposes', *Proc. 4th world conf. earthquake eng.*, 1969, pp. 145–160.
30. T. T. Soong, A. M. Reinhorn, Y. P. Wong and R. C. Lin, 'Full scale implementation of active control-part I: design and simulation', *J. struct. eng. ASCE* **117**, 3516–3536 (1991).
31. T. T. Soong, *Active Structural Control: Theory and Practice*, Longman Scientific and Technical, Wiley, New York, 1990.
32. J. N. Yang, A. Akbarpour and P. Gaemmaghami, 'New optimal control algorithms for structural control', *J. eng. mech. ASCE* **113**, 1369–1386 (1987).